



A novel pump-free ultrafiltration rate modulation system for continuous renal replacement therapy applications

Alessandra Ventresca^{1,2} · Guido Comai² · Stefano Severi¹

Received: 29 November 2022 / Accepted: 14 December 2022 / Published online: 30 January 2023
© The Author(s) 2023

Abstract

Purpose Extracorporeal ultrafiltration is an attractive alternative to diuretics for removing excess plasma water in critically ill patients suffering from fluid overload. In continuous renal replacement therapy (CRRT), ultrafiltration occurs in isolated form (SCUF) or supplemented by replacement fluid infusion (CVVH) and the net fluid removal rate is controlled by peristaltic pumps. In this work, a pump-free solution for regulating the ultrafiltration rate in CRRT applications is presented.

Methods The system consists of a motorized clamp on the ultrafiltration line, whose intermittent opening is modulated with a closed-loop control system based on monitoring of ultrafiltrate collected and any replacement fluid infused. The system was tested on two platforms for SCUF and CVVH, with “low-flux” and “high-flux” hemofilter, with various ultrafiltration setpoints and patient net weight loss targets.

Results In all configurations the set ultrafiltration rate was achieved with a maximum error of 5% and the values recorded were kept within ± 100 ml/h with respect to the setpoint, as recommended by international standard IEC 60601-2-16. The net fluid removal trend was highly correlated with that expected ($95\% < R^2 < 99\%$) and the weight loss target was reached in the expected time. For low ultrafiltration rates (60–150 ml/h) the system accuracy was better with the “low-flux” hemofilter.

Conclusion The developed clamp system represents a valid alternative to state-of-the-art solutions with peristaltic pumps in terms of performance, with potential usability advantages. The compliance with safety requirements given by international standard IEC 60601-2-16 is a prerequisite for clinical use.

Keywords Clamp · Pinch-valve · Slow continuous ultrafiltration · Hemofiltration · Net fluid removal · Fluid overload

1 Introduction

Fluid overload (FO) or hypervolemia is a common complication in critical patients suffering from acute kidney injury (AKI) and can be caused by excessive fluid administration or by worsening kidney disease [1–3]. Hypervolemia does not only indicate a renal impairment but is often associated with multi-organ dysfunction [4]. Several studies show that an

increase in body weight of more than 10% due to fluid retention increases the mortality rate and worsens the clinical condition of critical patients with respiratory failure, sepsis, or AKI [2, 5, 6]. In addition, more than 90% of hospitalizations for acute decompensated heart failure (ADHF) are due to fluid overload, with poor prognosis. Abnormal fluid retention begins in the early stage of heart failure and leads to physiological consequences involving other organs. The activation of neuro-humoral system promotes sodium retention, unbalanced hemodynamics, inflammation, and oxidative stress, affecting kidney functions in ADHF. The close interaction between heart and kidney, whereby a dysfunction in one organ is reflected on the other, is defined as cardio-renal syndrome (CRS) [7–10]. The removal of excess fluid becomes crucial in hypervolemic patients in such critical conditions. Diuretic agents are the first-line therapeutic strategy to relieve the symptoms of fluid overload. However, it is quite common that massive use of diuretics causes unresponsiveness of patients to drug treatment, with worsening

✉ Alessandra Ventresca
alessandra.ventresca2@unibo.it

Guido Comai
guido.comai@mediconingegneria.it

Stefano Severi
stefano.severi@unibo.it

¹ Department of Electrical, Electronic and Information Engineering “Guglielmo Marconi” (DEI), Alma Mater Studiorum University of Bologna, 40136 Bologna, Italy

² MediCon Ingegneria s.r.l, 40054 Budrio, Italy

the clinical condition [7–10]. In fluid overloaded patients not responding to diuretics, extracorporeal ultrafiltration proved to be a viable alternative to the pharmacological approach, where excess fluids are mechanically removed across the hemofilter membranes. Slow continuous ultrafiltration (SCUF) is a form of continuous renal replacement therapy (CRRT) specifically used to achieve patient weight loss by removing excess plasma water from whole blood [8, 11–13]. Low filtration rates (2–8 mL/min) are typically employed to fulfil the fluid removal target, with low blood flow rates and filters with a small surface area [14]. Clinical studies on ultrafiltration show that SCUF effectively reduces oedema and neurohormonal activation, improves hemodynamic balance and has beneficial effects on diuretics response. For patients requiring solute clearance in addition to fluid removal, and for a better volume control, ultrafiltration can be supplemented with simultaneous infusion of a sterile solution (continuous veno-venous hemofiltration, CVVH), [8, 15–17]. The replacement fluid may be administered upstream (pre-dilution) or downstream (post-dilution) of the blood filter. The post-dilution solution is more efficient at removing solutes, whereas the pre-dilution mode helps to reduce coagulation phenomena on the filter [15]. To increase the solute clearance, ultrafiltration rates typically used in CVVH are significantly higher than those of isolated ultrafiltration [16]. Given the importance of proper fluid balance in critical patients, CRRT devices must be equipped with precise net fluid removal control systems that considers the ultrafiltrate product and any fluid administered [18, 19]. In common practice the ultrafiltration process is driven by a peristaltic pump on the effluent compartment of the hemofilter [11–13, 20]. During treatment, the inevitable increase in blood viscosity due to hemoconcentration promotes coagulation phenomena, thus increasing the filter resistance. In addition, the progressive clogging of the porous membrane reduces its permeability. This causes the gradual increase in transmembrane pressure, which is therefore monitored with a pressure sensor on the effluent line [21–23]. In membrane conditions close to saturation and transmembrane pressure values dangerous to filter integrity, the main troubleshooting is to reduce the ultrafiltration rate setting, plan the replacement of the circuit, flush the filter with saline solution or even prematurely interrupt the treatment.

This work presents an alternative solution to drive the ultrafiltration process and control the net fluid removal rate in CRRT devices, intended for use in both isolated ultrafiltration and when replacement fluid infusion is needed. The ultrafiltration is controlled through the intermittent opening of a motorized clamp on the effluent line of the hemofilter, with no need for a peristaltic pump and a pressure sensor for transmembrane pressure measurement. A closed-loop control system is used to modulate the opening of the clamp and then the net fluid removal

rate, monitoring in real-time the amount of ultrafiltrate product and any replacement fluid infused through dedicated weight scales.

2 Materials and methods

2.1 Theoretical background

The ultrafiltration process is defined as the removal of plasma water (solvent, free of cells and colloids) from whole blood across a semipermeable membrane, driven by a transmembrane pressure (TMP) gradient between the blood and effluent compartments.

In continuous renal replacement therapy (CRRT) the ultrafiltration process takes place in the hemofilter, which consists of a bundle of hollow capillary fibers coated with a semi-permeable synthetic membrane made of a thin layer of porous plastic material, with specific characteristics of selective permeability to different solutes and water. The overall ultrafiltration rate UFR is defined as the ultrafiltrate volume produced per unit of time. In convective blood purification modalities such as CVVH, where ultrafiltration is performed in combination with replacement fluid infusion, the net ultrafiltrate rate (UFR_{net}) corresponds to the net volume of fluids removed from the patient by the machine per unit of time, so it is calculated as the difference between the overall UFR and replacement fluid infusion rate. In SCUF applications only fluid removal is provided, so UFR_{net} and UFR coincide.

The ultrafiltration rate is influenced by both operating parameters such as TMP and hemofilter intrinsic permeability properties.

The overall UFR [ml/h] can be calculated as [15]:

$$UFR = K_{uf} \times TMP$$

Where:

- K_{uf} = hemofilter ultrafiltration coefficient [ml/(h × mmHg)]
- TMP = transmembrane pressure [mmHg]

The transmembrane pressure can be approximated as [15, 16]:

$$TMP = \frac{P_{bi} + P_{bo}}{2} - P_{uf}$$

Where:

- P_{bi} = blood pressure at filter inlet.
- P_{bo} = blood pressure at filter outlet.
- P_{uf} = ultrafiltrate pressure at filter effluent line.

The membrane ultrafiltration coefficient (DK_{uf}) reflects the water permeability of the filter hollow fiber membranes per

unit pressure and surface. For any given filter, the ultrafiltration coefficient K_{uf} is the DK_{uf} multiplied by the membrane surface area of that filter (A). K_{uf} depends on both the dimensions of the membranes, the number of pores and pore dimensions. The unit of measurement is $[ml/(h \times mmHg)]$ [24, 25].

This parameter is provided by filter manufacturers, and it is measured experimentally as the ratio of the ultrafiltration rate UFR per unit of applied TMP:

$$DK_{uf} = \frac{UFR}{TMP} \times \frac{1}{A} \Rightarrow K_{uf} = \frac{UFR}{TMP}$$

Based on K_{uf} parameter, “low-flux” ($K_{uf} < 10$ ml/h/mmHg), “medium-flux” ($10 < K_{uf} < 25$ ml/h/mmHg) and “high-flux” ($K_{uf} > 25$ ml/h/mmHg) hemofilters are identified [15, 16].

The ultrafiltration rate for a given filter is directly proportional to transmembrane pressure, but the relationship is linear only within a certain pressure range, beyond which a plateau is reached. Leaning towards the curve plateau, any increase in TMP pressure becomes ineffective on the ultrafiltration rate [24–26]. This is due to the progressive reduction of filter performance. Indeed, the filter permeability is strongly affected by the fouling phenomenon, which is the deposition of plasma proteins on the membrane surface, leading filter to clog. The reduction in the number of pervious pores and the high oncotic pressure due to secondary protein layer opposes the ultrafiltration process.

2.2 State of the art

The early forms of CRRT devices consisted of arterio-venous blood circuits, where the patient’s own arterial pressure was used to pump the blood through the hemofilter, and the ultrafiltration rate was adjusted by manually lifting up the ultrafiltrate collection bag to the height. With the integration of roller pumps into the CRRT circuit, arterio-venous pressure gradients were no longer needed for flow rate generation in the extracorporeal circuit [8, 11–13]. In modern venovenous CRRT devices, roller pumps with adjustable flow-rate are used not only for blood circulation (blood pumps), but also for the infusion of replacement fluid (replacement pumps) and to guide the ultrafiltration process (ultrafiltration pump) [14]. Roller pumps on the ultrafiltration line are used to create a negative pressure in the ultrafiltrate compartment, and consequently to generate the transmembrane pressure gradient for the ultrafiltration process [12, 13, 20]. The variation in the flow rate of roller pumps makes it possible to modulate the extent of fluid removal by ultrafiltration and thus, ultimately, to control the patient’s weight loss [18]. Further, the ultrafiltrate product is monitored through weight scales connected to the fluid collection bag. To prevent circuit breakage from overpressure and reduce the risk of blood

loss, in CRRT devices internal pressures are monitored by appropriate sensors. For monitoring hemofilter-related pressures, the sensors are positioned at the inlet and outlet (differential pressure), and on the effluent line (transmembrane pressure) [22, 23].

2.3 Proposed solution operating principle

This work presents a pump-free system for the regulation of ultrafiltration in CRRT devices. Plasma water is removed by means of an intermittent and controlled opening of a motorized clamp on the effluent line of the hemofilter, acting as pinch-valve. With the clamp closed the effluent line is occluded, and the ultrafiltration is prevented in the absence of a transmembrane pressure gradient. When opening the pinch-valve, the hydrostatic pressure exerted by the vertical water column on the effluent line (P_{uf}) in the opposite direction acts as the driving force for the ultrafiltration process, contributing to the transmembrane pressure gradient across the hemofilter membranes. The height of the water column corresponds to the height distance between the outlet point of the effluent line on the hemofilter and the connection point with the ultrafiltrate collection bag. The ultrafiltration line pressure can be estimated according to the Stevin law:

$$P_{uf} = \rho \times g \times h$$

Where:

- P_{uf} = ultrafiltration line pressure [mmHg].
- ρ = water density = 1000 [kg/m³]
- g = gravitational acceleration = 9.81 [m/s²]
- h = height of water column [m].

Based on circuit layout (Fig. 1a, b) where $h = 1$ m, the ultrafiltration pressure P_{uf} given by water column is estimated to be 9810 Pa (~75 mmHg) on both SCUF and CVVH platforms.

The filter and the effluent line shall be airlessly primed before the treatment session with saline solution, to keep the pressure drop fixed and constant from the start of the ultrafiltration process.

In ultrafiltration phase the estimated transmembrane pressure gradient [mmHg] is:

$$TMP = P_b - P_{uf} = \frac{P_{in} + P_{out}}{2} - P_{uf}$$

Where:

- P_b : hydrostatic pressure on the blood compartment, intended as the average value between:
- P_{in} : pressure measured at the filter inlet.
- P_{out} : pressure measured at the filter outlet.
- P_{uf} : estimated hydrostatic pressure exerted by water column on the effluent line.

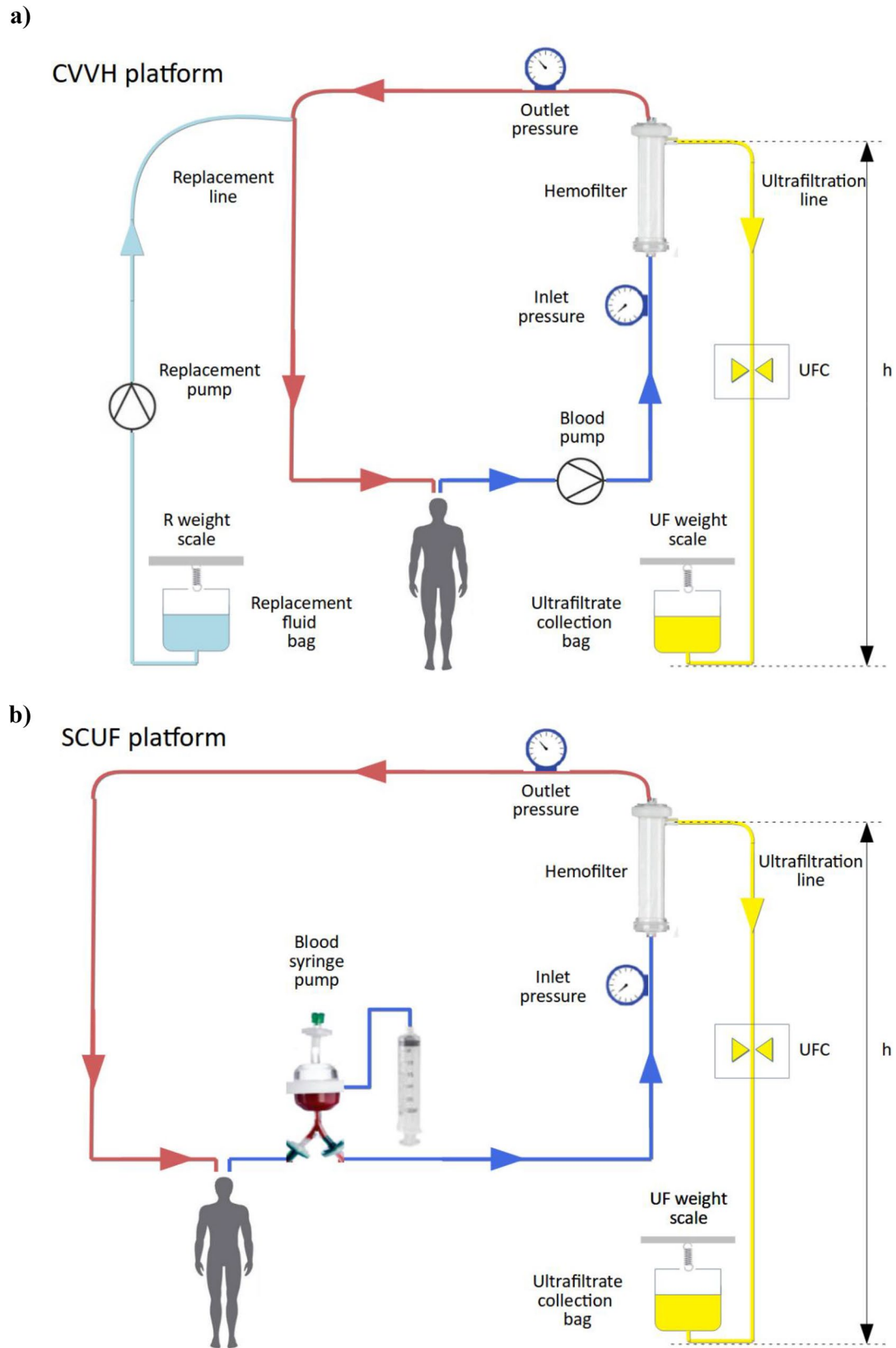


Fig. 1 **a** Schematic representation of the CVVH platform circuit. $h = 1$ m. **b** Schematic representation of the SCUF platform circuit. $h = 1$ m.

The intermittent opening of the clamp is modulated through a closed loop control system, with the aim to reach the target patient's weight loss while maintaining a desired net ultrafiltration setpoint. The final weight loss is then achieved by losing small amounts of fluid at each clamp opening over treatment time. To maintain the net ultrafiltration rate setpoint, the ultrafiltrate collected and any infused replacement fluid are monitored in real-time via weight scales and used as an input for the control system.

Therefore, the proposed ultrafiltration system is intended to be suitable for use in CRRT devices performing isolated ultrafiltration (SCUF) but also when simultaneous replacement fluid infusion is provided (CVVH): in both cases, the overall ultrafiltration rate is monitored to maintain the desired net fluid removal rate setpoint.

In SCUF application, the net ultrafiltration rate (*netUFR*) coincides with the overall ultrafiltration rate (*UFR*):

- $netUFR = UFR$.

In CVVH application, the net ultrafiltration rate also considers the replacement fluid infusion rate (*RFR*):

- $netUFR = UFR - RFR$

The control system provides real-time monitoring of the ultrafiltration rate. Based on weight data measured by scales, any excessive or insufficient variation in the net fluid removal rate compared to the desired setpoint, is detected. In compliance with international standard IEC 60601-2-16 [27] a protective system is also provided, independent of the control system to reduce the risk of uncontrolled ultrafiltration. Each intervention of the protective alarm system activates visual and audio signals and interrupts the ultrafiltration process. In addition, the weight data measurement chain provides intrinsic safety measures with redundant data acquisition channels from load cells.

2.4 Hardware design

The ultrafiltration system was built and tested on two CRRT platforms, one for isolated slow continuous ultrafiltration (SCUF), one for continuous hemofiltration (CVVH). In SCUF platform (Chiara, MediCon Ingegneria s.r.l., Budrio) the extracorporeal circuit included a “low-flux” hemofilter with small surface area ($S_{up} = 0.2 \text{ m}^2$, $K_{uf} = 7 \text{ ml/h/mmHg}$, blood flow range = 10–200 ml/min). A syringe-type blood pump was used with alternating, asymmetrical and continuous flow. For CVVH platform (CO2RESET, Eurosets s.r.l., Medolla) the tubing set was equipped with a “high-flux” hemofilter with a larger surface area ($S_{up} = 1.2 \text{ m}^2$, $K_{uf} = 55 \text{ ml/h/mmHg}$, blood flow range = 50–200 ml/min). Two

peristaltic pumps were used, one for blood flow (BLOOD PUMP) and the other for replacement fluid infusion (REPLACEMENT PUMP). The enabling of replacement line, inserted in post-dilution, was managed via the device user interface. The clamp movement was driven by a linear stepper motor (NIDEC SERVO, Model KH42JM2-951) operating on a cam mounted on the motor shaft. The cam acts on a sliding component by giving it an alternating motion: on one side there is the occlusion section, on the other side a pre-loaded spring is inserted. When the actuation system is powered to open the pinch-valve, the cam compresses the spring which increases its resistant force: the maximum resistant force corresponds to the maximum opening of the tube. When the system is not powered, the preloaded spring ensures the complete closure of the clamp (Fig. 2a). The motor is intended to be driven both in a clockwise or counterclockwise direction by a dedicated Stepper motor board (ULTRAFILTRATION CLAMP BOARD) and a power stage driver. The clamp was set up to ensure different degrees of tube occlusion: from complete flow obstruction (opening percentage = 0%) to free fluid passage (opening percentage = 100%). The control system is based on a microcontroller (uC Masterboard) that implements clamp opening modulation. Further, an optical “OPEN/CLOSED” sensor (OPTEK, Model OPB360T51 Slotted Optical Switch, Transmissive, Phototransistor Output) was used for real-time monitoring of the clamp opening status, and to detect any anomalous pinch-valve movement during ultrafiltration. The main components of the proposed solution are shown in the system block diagram (Fig. 2b). Ultrafiltrate collection bag and, in CVVH platform, also replacement fluid bag was hung to load cells for weight measurement and real-time monitoring of net fluid removal. Double channel load cells (Manufacturer: PICOTRONIK, Model: AAA-2 DOUBLE BRIDGE, Nominal load: 5 Kg, Sensitivity: $2.3 \pm 0.2 \text{ mV/V}$, zero balance: $\pm 0.02 \text{ mV/V}$, Creep: $\pm 0.5 \text{ uV/V}$, Abs. Error: $\pm 1\%$ nominal load) were used with the redundancy of strain gage sensors (resistive Wheatstone bridge). Furthermore, a non-invasive pressure sensing system was chosen for pre-filter and post-filter pressure monitoring. The μC boards of the system were connected through a serial line, with data transmission according to the RS485 communication protocol.

2.5 Clamp ultrafiltration software algorithm

For ultrafiltration rate modulation, the following algorithm was implemented on uC Masterboard firmware. The reference point of the algorithm is the desired hourly net ultrafiltration rate (fluid removal), expressed in ml/h, which is set via the device user interface and saved on a dedicated variable. The algorithm works with cycles of 60 s defined

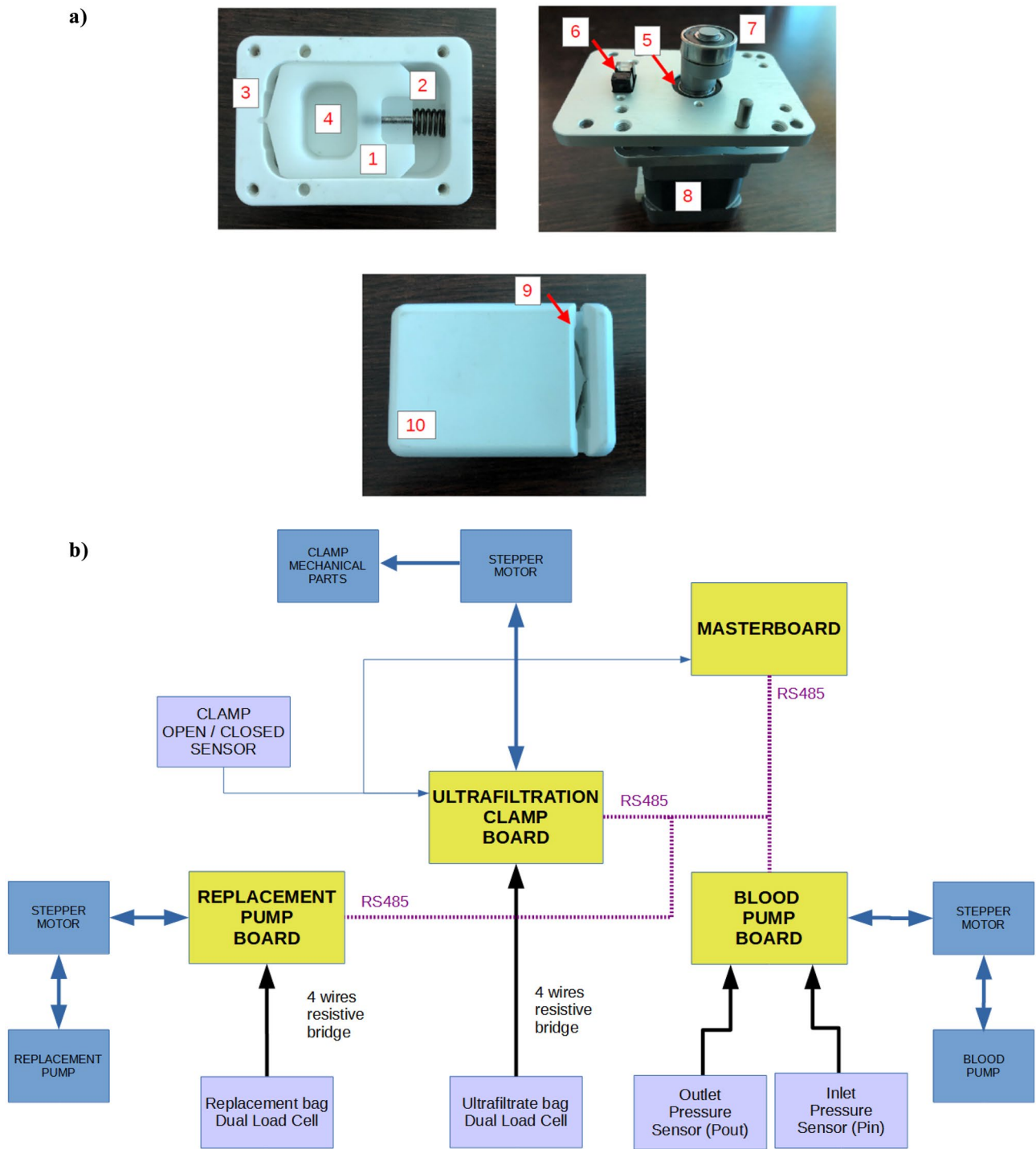


Fig. 2 **a** Mechanical parts of clamp element. 1) Sliding component 2) Pre-loaded spring 3) Occlusion section 4) Cam housing 5) Motor shaft 6) Optical sensor 7) Cam 8) Linear stepper motor 9) Ultrafiltration line housing 10) External enclosure in front view, **b** Block diagram of ultrafiltration rate modulation system

tion line housing 10) External enclosure in front view, **b** Block diagram of ultrafiltration rate modulation system

by timer τ . For each algorithm cycle, the clamp is opened for the time needed to produce the target amount of ultrafiltrate ($\Delta weight$) consistent with the hourly net ultrafiltration rate setpoint, monitored through load cells. When the

target of the current cycle is reached ($\Delta weight > target$), the pinch-valve is closed by interrupting the ultrafiltration process, and any excess weight loss (ERR) is stored and compensated in the next cycles. When the timer expires,

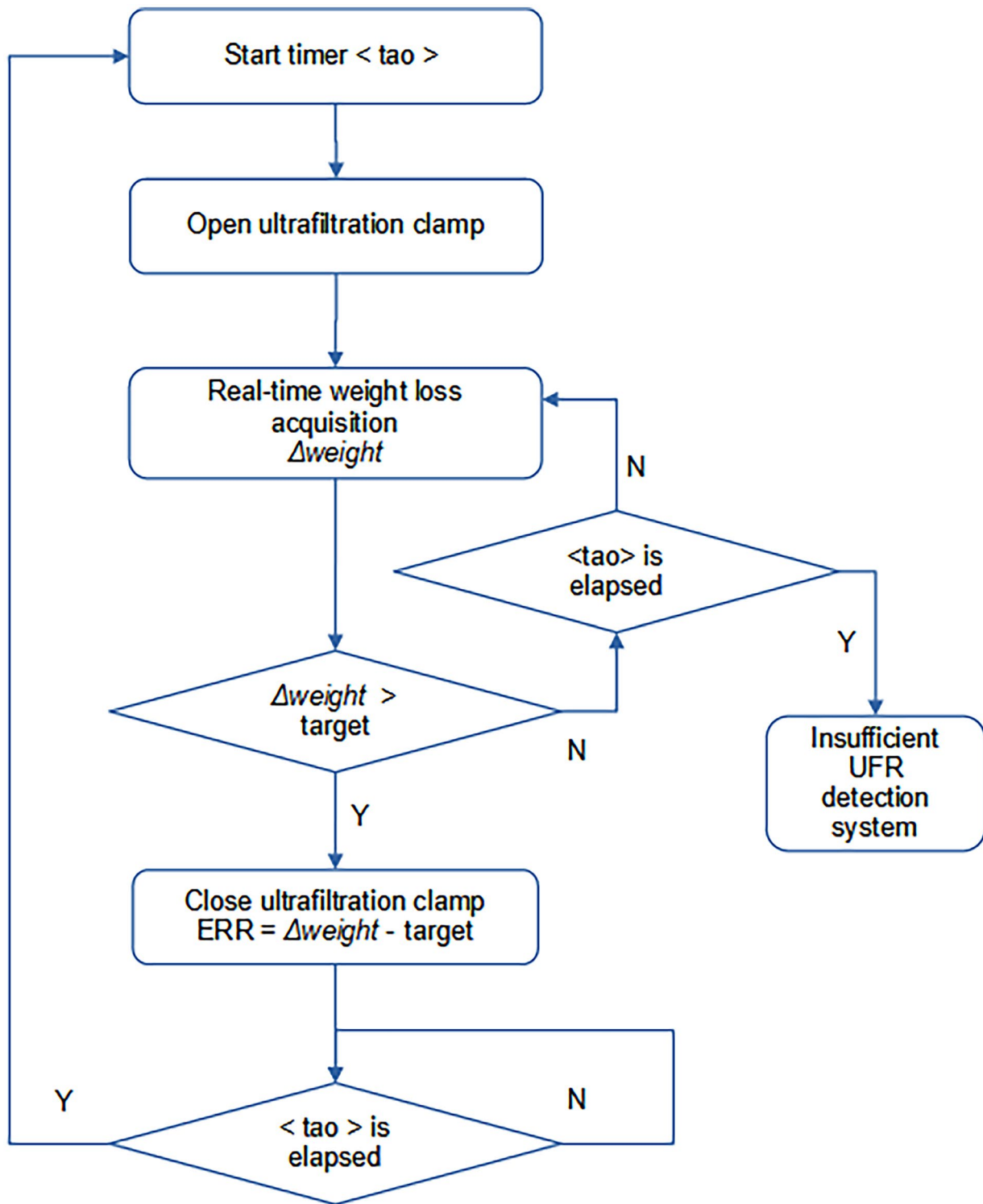


Fig. 3 Flowchart of ultrafiltration clamp modulation algorithm

a new cycle starts. If the target is not reached within the timer τ expiration, an insufficient ultrafiltration rate detection system is activated. In case of isolated ultrafiltration (SCUF platform), $\Delta weight$ coincides with the weight

increase of ultrafiltrate collection bag. In the presence of a replacement line (CVVH platform) the weight decrease of replacement bag is also considered. The total net fluid removed from the start of treatment is constantly monitored

and calculated as the sum of all “instantaneous” $\Delta weight$ of each cycle. A schematic simplified flowchart of the runtime algorithm implemented by Masterboard is reported in Fig. 3.

The control system for clamp opening modulation is also supplemented by dedicated functions for detection of any insufficient or excessive ultrafiltration rate through monitoring of weight variations on collection bags, and the related activation of visual and audio alarm.

2.6 Test protocol

The ultrafiltration system was tested on CVVH and SCUF platforms in two phases, a functionality test and an “in vitro” test.

The functionality test aimed to evaluate the ultrafiltration algorithm performance without external influences

due to fluid composition, in conditions of stable viscosity. For this reason, it was decided to use physiological solution, which being completely permeable to the hemofilter membranes does not change its viscosity during ultrafiltration process. Several configurations were tested, with different net ultrafiltration setpoints and replacement fluid infusion rates. The tests were carried out simulating treatment sessions with a minimum duration of 60 min, three repetition for each configuration (Test 1, 2, 3). Then, the ultrafiltration system was tested “in vitro” through 6-hour treatment sessions with bovine blood samples, to evaluate the system’s response to gradual hemoconcentration due to the removal of plasma water. The ultrafiltration algorithm variables and weight data received from load cells uC boards (Ultrafiltrate bag weight, Replacement bag weight) were displayed and monitored in real-time on the device user interface and stored on the device’s internal memory

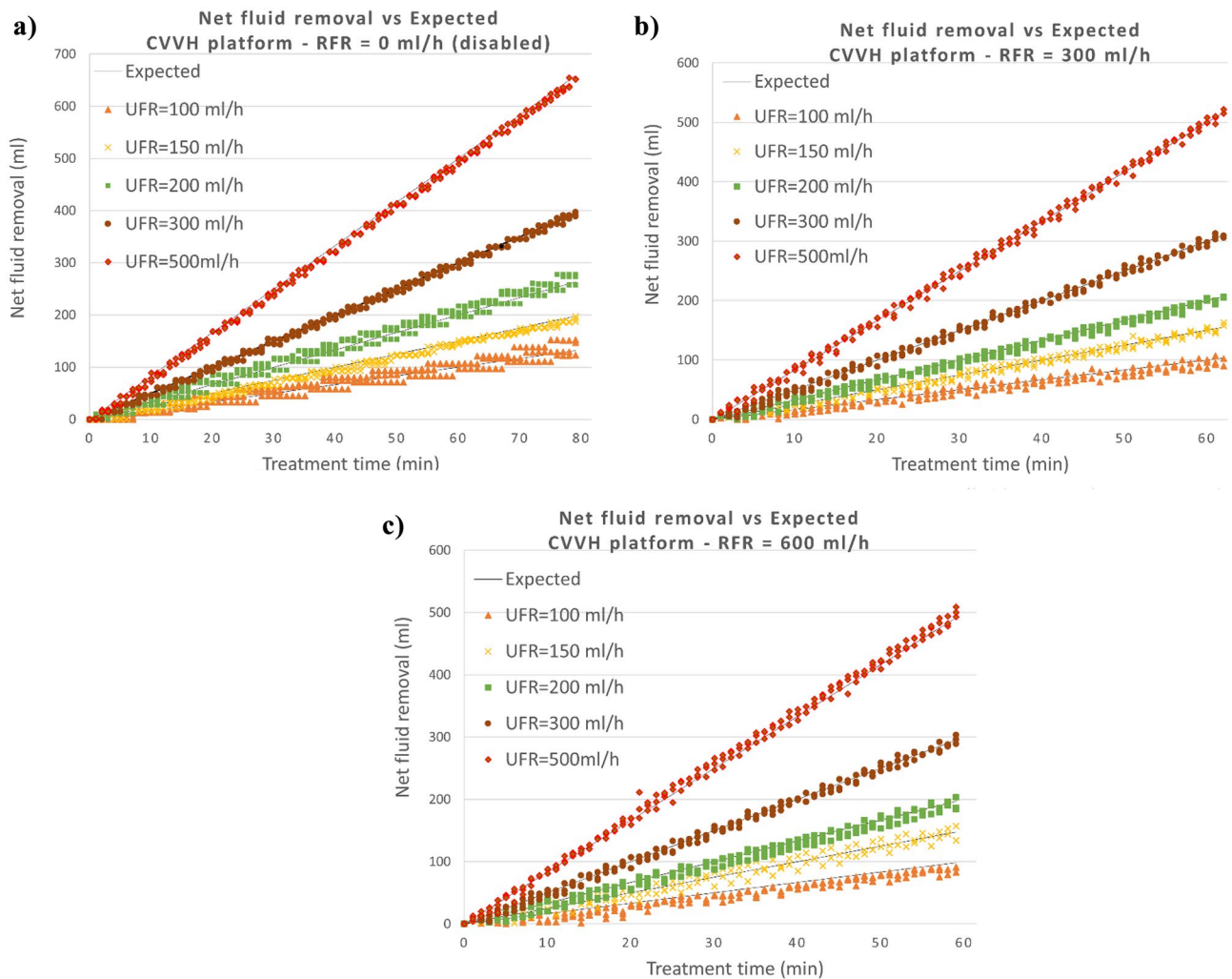


Fig. 4 Net fluid removal trends related to functionality tests on CVVH platforms for each tested configuration. UFR = net Ultrafiltration rate (ml/h); RFR = Replacement fluid infusion rate (ml/h). The

trends show the measured values (colored bullets) compared to the expected ones (black lines). **a** RFR = 0 ml/h, **b** RFR = 300 ml/h, **c** RFR = 600 ml/h

with a sampling frequency of one sample per minute for post-processing analysis.

3 Results

3.1 Functionality test

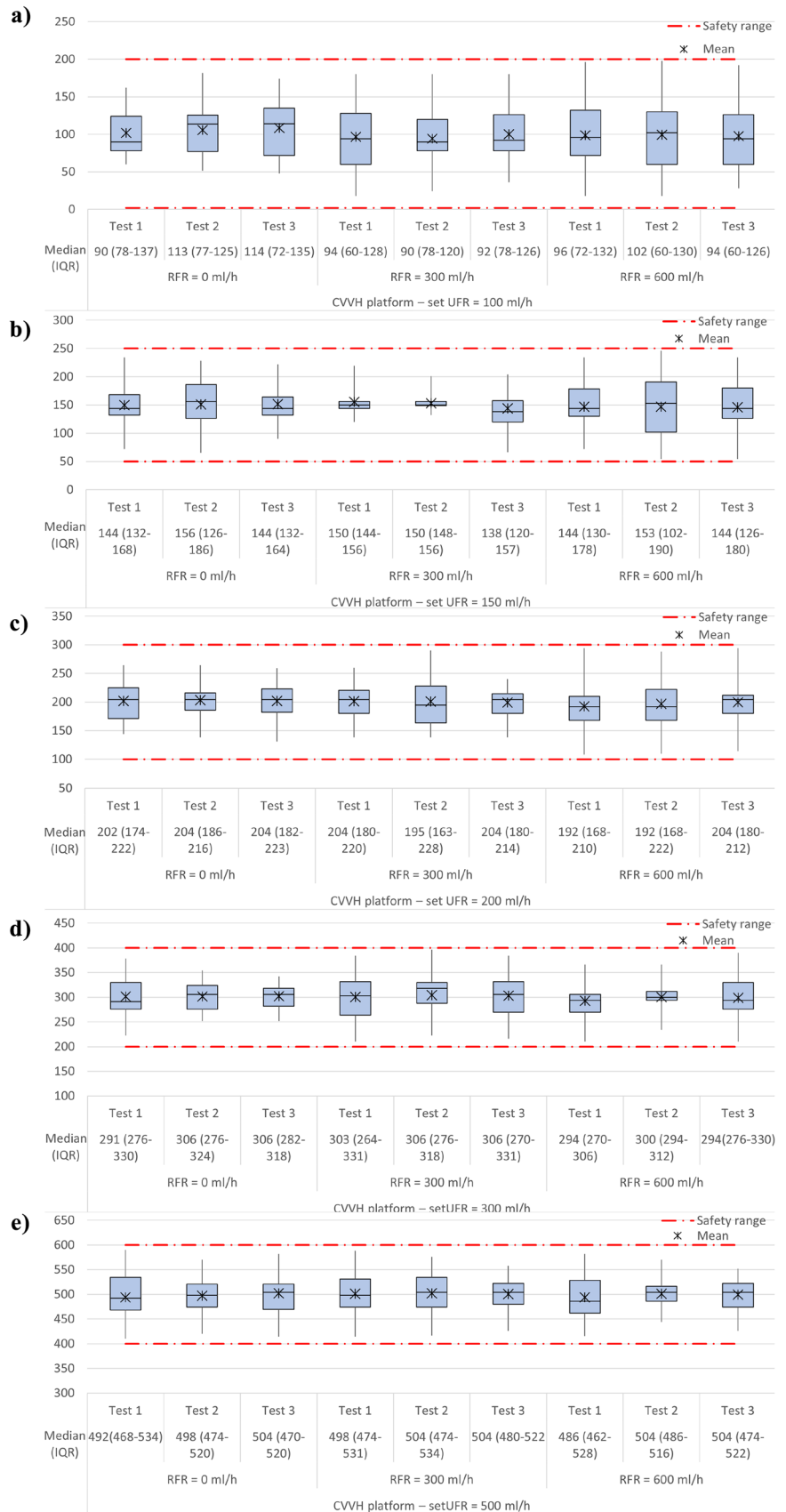
On CVVH platform the following setpoints of net ultrafiltration rate (*setUFR*) were tested: 100, 150, 200, 300, 500 ml/h. Each *setUFR* condition was verified with three replacement fluid rates (*RFR*): 0 (replacement line disabled), 300, and 600 ml/h, resulting in overall ultrafiltration rates ranging from 100 to 1100 ml/h. The graphs in Fig. 4 show all the net fluid removal values (weight loss) recorded during treatment sessions compared to the expected ones. Given the sampling frequency of the weight data from load cells (one sample/minute), the expected value for each elapsed minute was calculated as: *Expected [ml] = netUFR setpoint [ml/min] / Elapsed treatment time [min]*. In Table 1 the agreement between the measured net fluid removal and the expected one is reported in terms of linear regression (coefficient of determination R^2) and mean error (+/- 95% confidence interval). In all configurations, the linear regression process returns an R^2 index greater than 0.94, and the mean error range is $-10 \text{ ml} \div 12 \text{ ml}$. Based on weight data sampled from load cells, the “instantaneous” ultrafiltration rate was calculated every minute as $\Delta \text{weight} [\tau] / \tau$, where $\Delta \text{Weight} [\tau]$ is the weight increment measured in time interval τ , and τ is the sampling time = 60 s. The net ultrafiltration rate (*netUFR*) was averaged with a moving average filter of 10 samples. The boxplot diagrams in Fig. 5 show the distribution of sliding average net ultrafiltration rate (*netUFR*) values during treatment. In all configurations, there are no significant differences between the interquartile ranges of the repeated sessions (Test 1, 2, 3) and the median values are always close to the setpoint (+/- 15 ml/h), suggesting the high repeatability of the ultrafiltration system. Further, all the values including maximum and minimum are within $\pm 100 \text{ ml/h}$ with respect to the setpoint, as recommended by IEC 60601-2-16 standard (*Subclause 201.12.4.4.103 NET FLUID REMOVAL*) [27]. In Table 1 the overall net ultrafiltration rates (mean μ +/- standard deviation σ) are reported, calculated as the average of all *netUFR* moving average values. In all configurations, the percentage error of the average net ultrafiltration rate compared to the setpoint is always less than 5%. The standard deviations of net ultrafiltration values are within $30 \div 55 \text{ ml/h}$, with no significant differences between configurations. These results confirm the reliability of the developed ultrafiltration system in all tested configurations.

On the SCUF platform the following ultrafiltration setpoint were tested: 60, 100, 150, 200, and 500 ml/h. The

Table 1 – Functionality test: CVVH platform results

UFR set-point (ml/h)	100			150			200			300			500		
	0	300	600	0	300	600	0	300	600	0	300	600	0	300	600
Mean \pm SD (ml/h)	105 \pm 33	97 \pm 37	98 \pm 42	150 \pm 38	152 \pm 31	146 \pm 49	202 \pm 30	201 \pm 36	195 \pm 55	301 \pm 30	302 \pm 38	297 \pm 32	497 \pm 41	501 \pm 39	496 \pm 41
Final Error (%)	4.94	-3.17	-1.41	0.03	1.47	-2.72	1.17	0.32	-2.41	0.51	0.83	-0.92	-0.57	0.25	-0.82
Net fluid removal vs. Expected															
R^2	0.95	0.97	0.97	0.99	0.99	0.98	0.99	0.99	0.99	0.99	0.99	0.99	0.99	0.99	0.99
Mean error	12.15	-3.29	-10.41	-4.94	-2.46	-4.89	4.29	-1.37	-2.67	-2.44	-1.49	-0.41	-7.87	-0.10	5.91
(95% CI)	(-14.27, 38.58)	(-8.43, 1.86)	(-20.16, 0.66)	(-11.42, 1.55)	(-11.04, 6.12)	(-14.77, 5.00)	(-1.46, 10.03)	(-7.84, 5.11)	(-15.34, 10.00)	(-7.26, 2.38)	(-6.97, 4.00)	(-5.48, 4.66)	(-14.23, -1.52)	(-6.15, 5.95)	(-1.59, 13.40)

Fig. 5 Boxplots diagrams related to functionality tests on CVVH platform for each tested configuration. UFR = net Ultrafiltration rate (ml/h); RFR = Replacement fluid infusion rate (ml/h). The diagrams show the distribution of sliding average net ultrafiltration values (netUFR). The mean, the median value and the interquartile range (IQR) within first and third quartiles are reported. The safety range (red dashed lines) is that recommended by the EN 60601-2-16 standard (+/-100 ml/h with respect to the setpoint). For each net ultrafiltration rate (UFR) setpoint three test results (Test 1, 2, 3) are reported at different replacement fluid infusion rates (RFR =0 ml/h, RFR =300 ml/h, RFR =600 ml/h). **a** UFR =100 ml/h, **b** UFR =150 ml/h, **c** UFR =200 ml/h, **d** UFR =300 ml/h, **e** UFR =500 ml/h



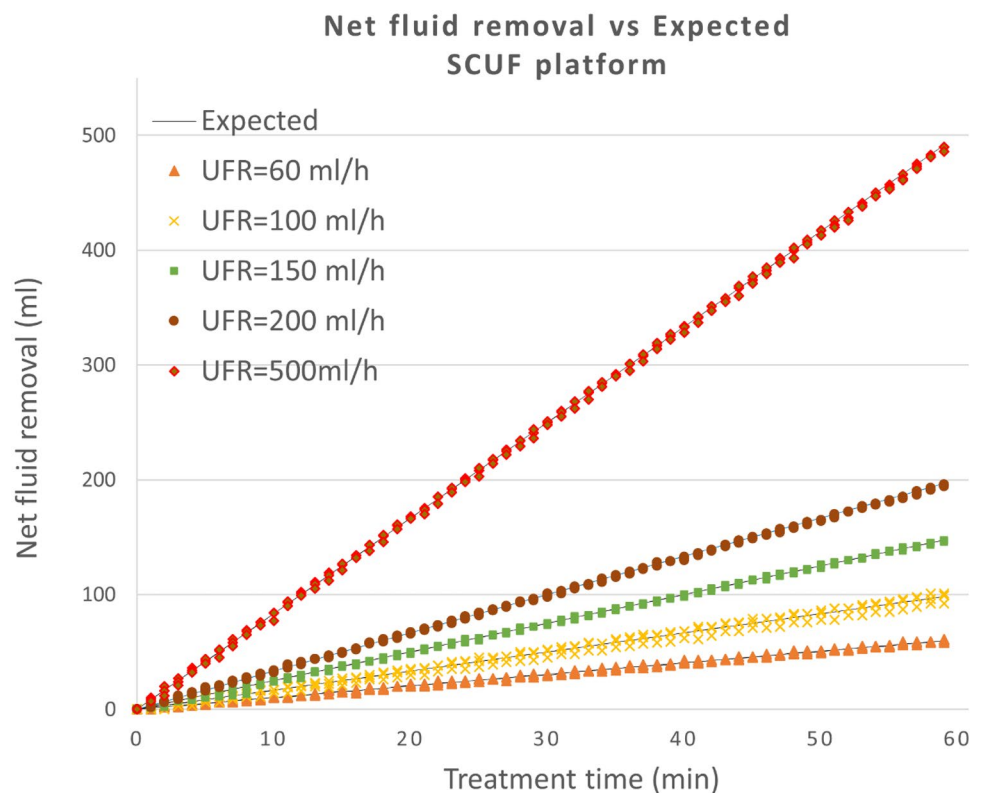
results related to the SCUF platform are reported in Table 2; Figs. 6 and 7. The R^2 index resulting from linear regression is always higher than 0.95 and the mean error range is $-2,5 \div 0$ ml, as confirmed by the net fluid removal trend (Fig. 6). Even on the SCUF platform (Fig. 7), the box plots related to *netUFR* moving average values highlight the repeatability of the ultrafiltration system and compliance with the IEC 60601-2-16 standard recommendations. The median values \pm IQR are within ± 15 ml/h with respect to the setpoint. Further, Table 2 shows that in all configurations the percentage error of the overall net ultrafiltration rate is always less than 2%, with a standard deviation σ within the range $5 \div 12$ ml/h. These results demonstrate a slightly higher accuracy in the SCUF platform compared to the CVVH platform and a lower variability of net ultrafiltration values, meaning a better precision in terms of net fluid removal trend over treatment time.

3.2 “In vitro” test

The “in vitro” tests of the developed ultrafiltration system were carried out on the hemofiltration line of CO2RE-SET device (Eurosets Srl, Medolla) with a high flux hemofilter (Sup = 1.2 m², Kuf = 55 ml/h/mmHg, blood flow range = 50–200 ml/min). Bovine blood samples (HCT = 32%) were used for the tests. Two treatment sessions were performed, setting the desired net ultrafiltration

rate and the overall net fluid removal target, based on which the expected treatment duration was estimated. For the first session, the net ultrafiltration rate was set to 100 ml/h, with a weight loss target of 600 ml. For the second session, the net ultrafiltration rate setpoint was 300ml/h, with a weight loss target of 1800 ml. In both cases, the estimated treatment time resulted to be 6 h. In the first 3 treatment hours an isolated ultrafiltration treatment was performed, with the replacement line disabled. In the following 3 h, the replacement line was enabled with a reinfusion flowrate of 600 ml/h. The hemofiltration line pump flowrate was kept within the functional range of 150–200 ml/min. In both sessions the target weight loss was reached in the estimated time (6 h) and net fluid removal trend was always consistent with the expected one (Fig. 8). Indeed, the regression analysis results in an R^2 of 0.99, with a mean error (\pm 95% CI) of -1 (-22 – 19) ml at 100 ml/h, and -2 (-10 – 6) ml at 300 ml/h. The results in Table 3 and the box plots in Fig. 8 show that the net ultrafiltration rate was always kept consistent with the setpoint. In the 100 ml/h test, the overall net ultrafiltration value (mean \pm standard deviation) is 99 ± 31 ml/h with a percentage error of less than -2% . In the 300 ml/h test, the overall net ultrafiltration (mean \pm standard deviation) is 299 ± 27 ml/h with a percentage error of less than -1% . The median values (IQR) of the distribution boxes are respectively 96(69–120) ml/h and 300 (288–312) ml/h. The IQR ranges highlight a greater variability of the values in

Fig. 6 Net fluid removal trends related to functionality tests on SCUF platform for each tested configuration. UFR = net Ultrafiltration rate (ml/h). The trends show the measured values (colored bullets) compared to the expected ones (black lines)



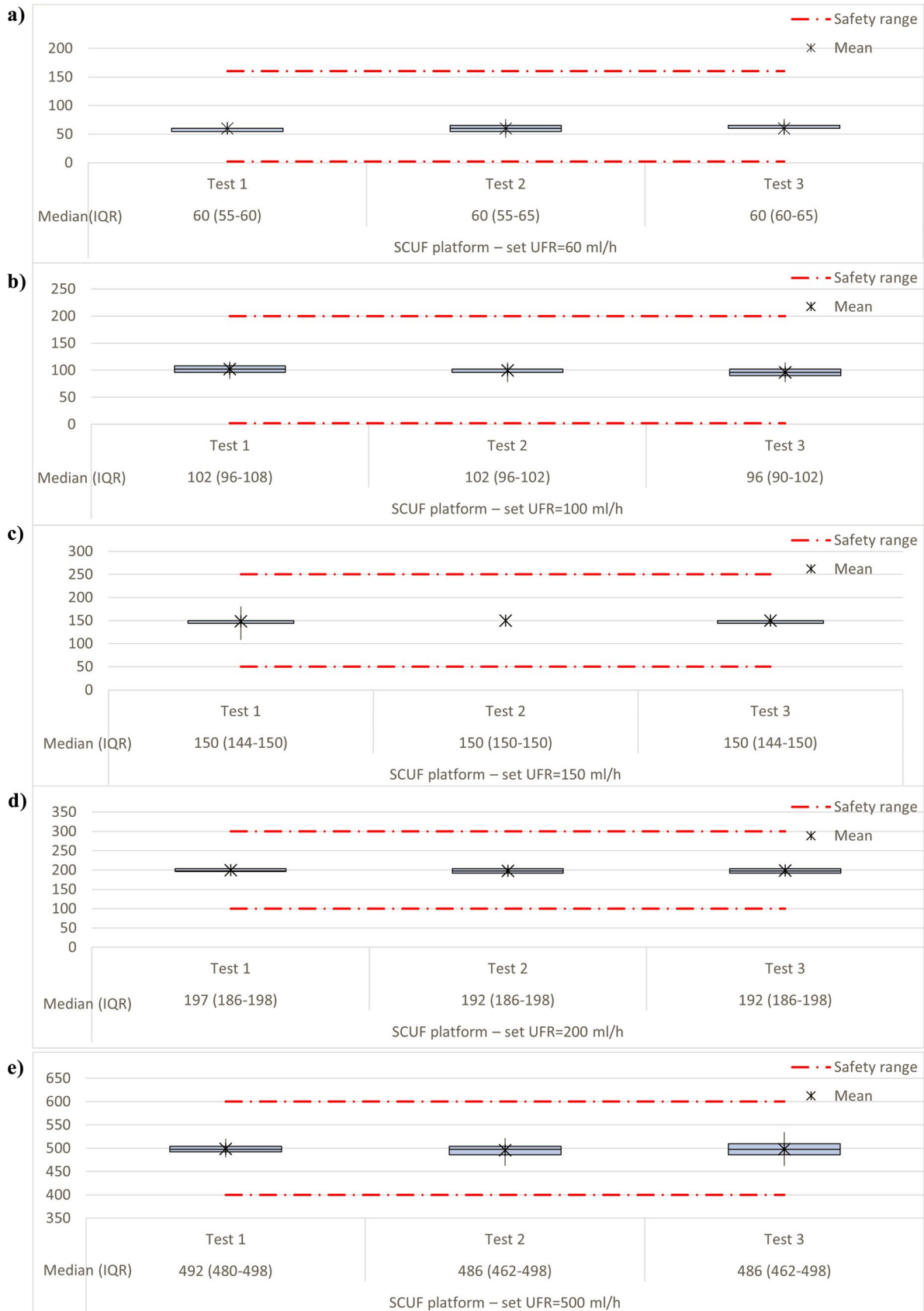


Fig. 7 Boxplots diagrams related to functionality tests on SCUF platform for each tested configuration. UFR = net Ultrafiltration rate (ml/h). The diagrams show the distribution of sliding average net ultrafiltration values (netUFR). The mean, the median value and the interquartile range (IQR) within first and third quartiles are reported. The safety range (red dashed lines) is that recommended by the EN 60601-2-16 standard (+/-100 ml/h with respect to the setpoint). For each net ultrafiltration rate (UFR) setpoint three test results (Test 1, 2, 3) are reported. **a** UFR =60 ml/h, **b** UFR =100 ml/h, **c** UFR =150 ml/h, **d** UFR =200 ml/h, **e** UFR =500 ml/h

the 100 ml/h test. The distribution boxes show that during treatment sessions the *netUFR* ultrafiltration rate values was always compliant with the safety range recommended by the IEC 60601-2-16 standard.

4 Discussion

In this work a system for the regulation of net ultrafiltration rate was presented, which is suitable for convective continuous renal replacement therapy (CRRT) applications as slow continuous ultrafiltration (SCUF) and continuous veno-venous hemofiltration (CVVH). The solution consists of a motorized clamp on the hemofilter effluent line and it is proposed as an alternative to the peristaltic pump, which is the state-of-the-art approach for CRRT devices.

The clamp opening is modulated through a closed loop control system based on real-time measurement of the amount of ultrafiltrate product and any fluid replacement infused, thanks to the use of weight scales on collection bags. The ultrafiltration mechanism, activated only when the pinch-valve is opened, is guided passively by the pressure drop on the effluent line. The water column creates the transmembrane pressure gradient needed to remove plasma water, thus avoiding the use of a dedicated pump.

The first evidence from functionality test is the high repeatability of the results, which suggests the reliability of the ultrafiltration system. Regardless of the net ultrafiltration rate set point, the ultrafiltration coefficient of the hemofilter (*K_{uf}*), the presence of the reinfusion line and the fluid viscosity, the net fluid removal trend followed the expected one with high agreement. Further, in all test conditions the set ultrafiltration rate was kept consistently. These

high performances were supported by “in vitro” tests with blood samples, and for both the ultrafiltration rate setpoint (100, 300 ml/h) the patient’s target weight loss (overall net fluid removal) was reached in the estimated treatment time (6 hours). On the SCUF platform, the system resulted to be more precise than the CVVH one, with smaller fluctuations in sliding average net ultrafiltration rate values over treatment duration. The net fluid removal trend was highly correlated to the expected one, with a negligible mean error on all the sampled values. Under the same treatment conditions, i.e., with the reinfusion line disabled (isolated ultrafiltration) on the CVVH platform, a “stepped” behavior of net fluid removal trend for low ultrafiltration rates (100–150 ml/h) was observed. This effect was found to decrease progressively with the increase of ultrafiltration setpoint, until disappearing at the maximum rate of 500 ml/h. With the reinfusion line enabled on the CVVH platform, the stepped effect was not shown for any of the tested setpoints. These results can be explained if we consider that, as an intrinsic characteristic of the developed system, the hydrostatic pressure exerted by the water column on the effluent line depends only on the ultrafiltration line-height distance. Since the height is the same in both platforms, with the same driving force across the hemofilter membranes the ultrafiltration rate is only affected by the permeability characteristics of the hemofilter. Therefore, on the CVVH platform the ultrafiltration process is expected to be faster than the SCUF, due to the larger surface area and a higher ultrafiltration coefficient of the hemofilter (“high-flux” vs “low-flux”). This implies that for low ultrafiltration setpoints, at each clamp opening the excess weight loss compared to the target was higher than on the SCUF platform, as demonstrated by the mean error data reported in Tables 1 and Table 2. However, the error was compensated by the software algorithm by keeping the clamp closed in the next cycles, causing a stepped weight loss. In the presence of a replacement line, the error was also compensated by continuous fluid re-infusion, so the stepped effect did not occur. The excess weight at pinch-valve opening also explains the greater fluctuations of sliding average ultrafiltration rate in CVVH platform.

Despite the variability, in all the conditions the system complies with the recommendations of the IEC 60601-2-16

Table 2 Functionality test: SCUF platform results

UFR setpoint (ml/h)	60	100	150	200	500
Mean ± SD (ml/h)	60 ± 5	99 ± 7	149 ± 7	199 ± 6	498 ± 12
Final Error (%)	0,12	-0,66	-0,36	-0,78	-0,50
Net fluid removal vs. Expected					
R ²	0,99	0,99	0,99	0,99	0,99
Mean error	0	-0.81	-0.67	-0.65	-2.36
(95% CI)	(-1.78, 1.78)	(-7.89, 6.27)	(-2.74, 1.41)	(-2.82, 1.52)	(-8.04, 3.32)

Table 3 “In vitro” test: CVVH platform results

UFR setpoint (ml/h)	100	300
Mean \pm SD (ml/h)	99 \pm 31	299 \pm 27
Final Error (%)	-1.42	-0.27
Net fluid removal vs. Expected		
R ²	0,99	0,99
Mean error	-1.30	-2.20
(95% CI)	(-21.82, 19.12)	(-10.32, 5.90)

standard, as the values remain largely within the recommended safety range of ± 100 ml/h with respect to the desired setpoint. This safety limit on the standard was established on the basis of clinical experience on devices for hemofiltration with net fluid removal and given as parameter to be considered for manufacturers. Therefore, the full compliance with the standard implies that the efficiency of the developed system is in line with hemofiltration devices in medical industry and it has prerequisites for clinical use.

Further, due to intrinsic implementation features the system may overcome some limitations related to roller pumps with potential benefits. One of the main drawbacks of peristaltic pumps is that the flow rate is maintained even with an increase in preload resistance [28, 29]. Therefore, when the hemofilter resistance increases due to membrane fouling, maintaining the ultrafiltration rate inevitably may cause an increase in transmembrane pressure. For this reason, a pressure sensor on ultrafiltration line is used as a monitoring system in hemofiltration devices to prevent internal pressures from reaching dangerous values for the integrity of the filter [12]. In critical clogging conditions, continuous operator intervention may be required to contain the pressure increase, by reducing the ultrafiltration rate or flushing the filter [21]. A rupture of the filter membranes could in fact lead to a premature interruption of the treatment, resulting in patient blood loss. In the proposed solution there are no active forces on the ultrafiltration line, but the ultrafiltration process is driven by the small and constant gravitational force, reducing stress on filter fibers. As hemoconcentration progresses during treatment, the membrane fouling can be compensated by increasing the opening times of the clamp to reach the fluid removal target with no excessive strain, preserving the integrity of the membrane fibers and thus potentially extending the filter’s functional life. In severe clogging conditions, where the compensation mechanism is no longer sufficient, treatment could be continued at a lower ultrafiltration rate, avoiding premature interruptions. As mentioned by IEC 60601-2-16 standard [27] an ultrafiltration rate below the setpoint is not considered a hazardous

situation for the patient. Therefore, continuing treatment at lower rates may be a good compromise to maintain the clinical benefit of ultrafiltration.

The system may also offer a greater control over transmembrane pressure, as it acts only during opening phase of the clamp. Therefore, the transmembrane pressure value is not a critical functional parameter and there is no need to use a pressure sensor for monitoring. This solution implies some advantages in terms of usability and costs reduction.

The use of a single open/closed pinch-valve instead of a group of components (pump and pressure sensor) is cheaper and simpler by construction and also the tubing set is simplified. The circuit setup procedure is therefore easier for the user, as it consists only in the insertion of the tube in the pinch-valve housing instead of the mounting of the sub-pump section and the pressure sensing system. Further, a pressure sensor must be periodically calibrated by the user and a peristaltic pump needs periodic cleaning. This maintenance intervention are not necessary with the use of a pinch-valve. The clamp system is also extremely noiseless compared to a peristaltic pump: this aspect may be significant for CRRT therapies in which long-term treatments are performed and the device is kept close to the critically ill patient. All these advantages are not at the expense of safety. The absence of transmembrane pressure sensing does not prevent to monitor filter clogging phenomena, which can be detected using the weight variation data of the ultrafiltrate collection bag.

This work has some limitations that could be overcome with further studies or developments. In the current modulation algorithm, only two opening percentages (0-100%) are used, leading to intermittent ultrafiltration. The algorithm could be further developed with a finer adjustment of the opening percentage, taking advantage of the entire opening range available. Partial clamp openings and a gradual adjustment could lead to a greater control over the ultrafiltrate production and therefore to a greater accuracy of the system. This solution could improve the stepped effect observed with small ultrafiltration setpoints in CVVH platform. Moreover, the system could be tested in the future also for diffusive CRRT modalities, that is in presence of a countercurrent dialysate in the effluent compartment of the hemofilter.

In conclusion, in this work a pump-free ultrafiltration system for the regulation of the net ultrafiltration rate in CRRT devices was presented. The results showed that it is an effective alternative to the state-of-the-art solutions with peristaltic pumps and may offer potential advantages in terms of usability. The high efficiency and reliability of the system and compliance with international regulations for hemofiltration equipment in terms of safety suggest the potential use in clinical practice.

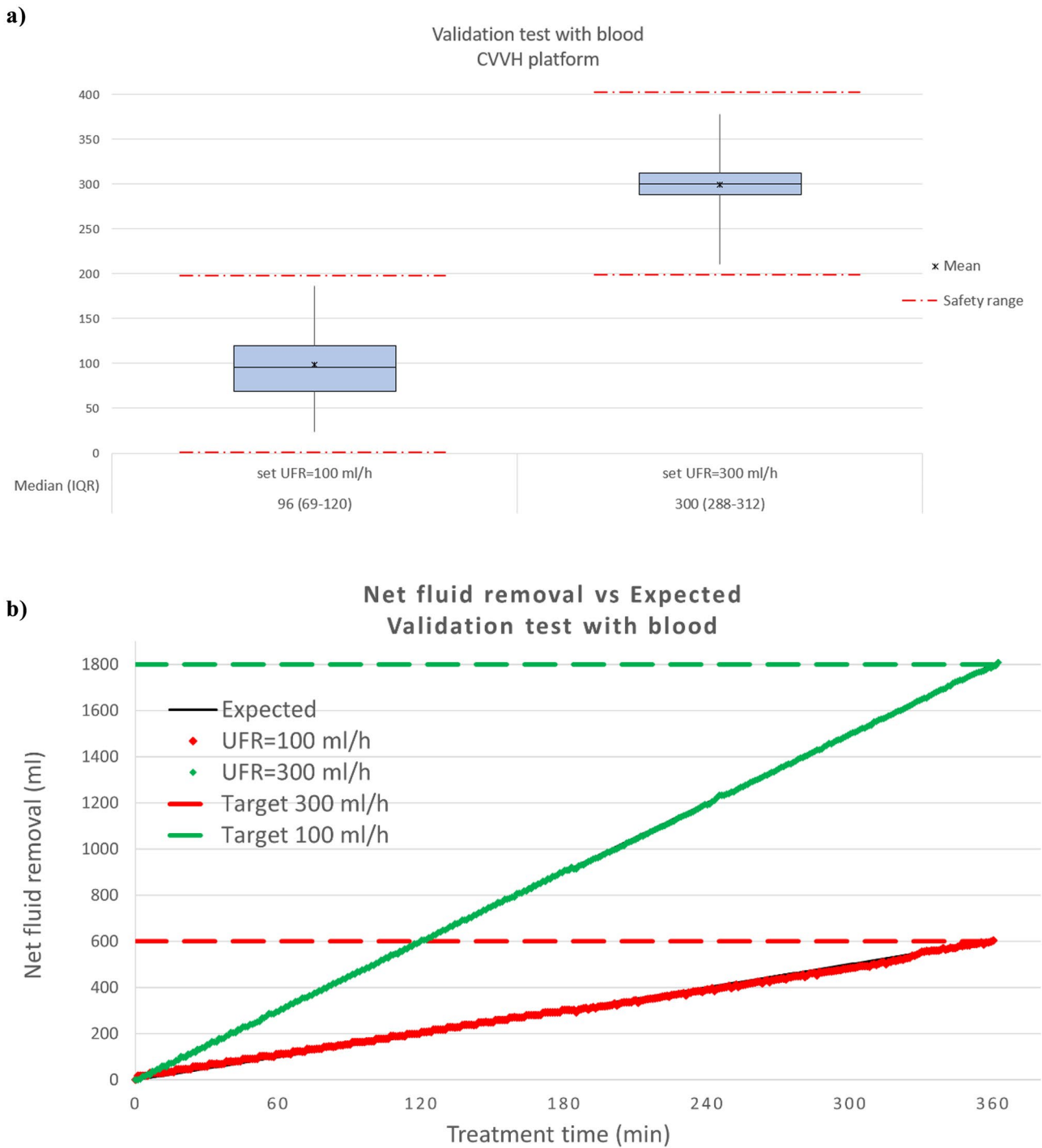


Fig. 8 Boxplots diagrams and Net fluid removal trends related to “in vitro” tests on CVVH platforms at 100 ml/h and 300 ml/h. UFR = net Ultrafiltration rate (ml/h); RFR = Replacement fluid infusion rate (ml/h). **a)** The diagrams show the distribution of sliding average net ultrafiltration values (netUFR). The mean, the median value and the

interquartile range (IQR) within first and third quartiles are reported. The safety range (red dashed lines) is that recommended by the EN 60601-2-16 standard (+/-100 ml/h with respect to the setpoint). **b)** The trends show the measured values (colored bullets) compared to the expected ones (black lines)

Acknowledgements The authors would like to acknowledge Eurosets s.r.l. for providing laboratory equipment for “in vitro” test with blood using CO2RESET device.

Author contributions Conceptualization, A.V. and G.C.; methodology, A.V. and G.C.; software, A.V. and G.C.; writing—original draft, A.V., writing—review and editing, A.V., G.C. and S.S.; supervision, S.S. All authors have read and agreed to the published version of the manuscript.

Funding Open access funding provided by Alma Mater Studiorum - Università di Bologna within the CRUI-CARE Agreement. This research was sponsored by MediCon Ingegneria s.r.l.

Declarations

Conflict of interests S.S. declares no conflict of interest. A.V. is a full-time employee at MediCon Ingegneria s.r.l., in the framework of a PhD Apprenticeship Program at University of Bologna, G.C. is Technical Director and Co-Owner of MediCon Ingegneria s.r.l.

Open Access This article is licensed under a Creative Commons Attribution 4.0 International License, which permits use, sharing, adaptation, distribution and reproduction in any medium or format, as long as you give appropriate credit to the original author(s) and the source, provide a link to the Creative Commons licence, and indicate if changes were made. The images or other third party material in this article are included in the article's Creative Commons licence, unless indicated otherwise in a credit line to the material. If material is not included in the article's Creative Commons licence and your intended use is not permitted by statutory regulation or exceeds the permitted use, you will need to obtain permission directly from the copyright holder. To view a copy of this licence, visit <http://creativecommons.org/licenses/by/4.0/>.

References

- Hall A, Crichton S, Dixon A, Skorniakov I, Kellum JA, Ostermann M. Fluid removal associates with better outcomes in critically ill patients receiving continuous renal replacement therapy: a cohort study. *Crit Care BioMed Central*. 2020;24:279.
- Claire-Del Granado R, Mehta RL. Fluid overload in the ICU: evaluation and management. *BMC Nephrol*. BioMed Central Ltd. 2016.
- Kim IY, Kim JH, Lee DW, Lee SB, Rhee H, Seong EY, et al. Fluid overload and survival in critically ill patients with acute kidney injury receiving continuous renal replacement therapy. *PLoS One Public Lib Sci*. 2017;12.
- Yerram P, Karuparthi PR, Misra M. Fluid overload and acute kidney injury. *Hemodialysis Int*. 2010;348–54.
- Joannidis M, Forni LG, Klein SJ, Honore PM, Kashani K, Ostermann M, et al. Lung–kidney interactions in critically ill patients: consensus report of the Acute Disease Quality Initiative (ADQI) 21 Workgroup. *Intensive Care Med*. Springer 2020;46:654–72.
- Husain-Syed F, Slutsky AS, Ronco C. Lung-kidney cross-talk in the critically ill patient. *Am J Respir Crit Care Med*. 2016;402–14.
- Marenzi G, Morpurgo M, Agostoni P. Continuous Ultrafiltration in Acute Decompensated Heart failure: current issues and future directions. *Am J Cardio Drugs*. Springer International Publishing 2015;103–12.
- Nalesso FGFRC. Technical aspects of extracorporeal ultrafiltration - mechanisms, monitoring and dedicated technology.pdf-annotated. *Contrib Nephrol*. 2010;164:199–208.
- Jentzer JC, Bihorac A, Brusca SB, del Rio-Pertuz G, Kashani K, Kazory A, et al. Contemporary Management of Severe Acute Kidney Injury and Refractory Cardiorenal Syndrome: JACC Council Perspectives. *J Am Coll Cardiol*. Elsevier Inc. 2020;1084–101.
- van der Eijk Y, Ng XY, Lee JK. Pathophysiology of Cardiorenal Syndrome and Use of Diuretics and Ultrafiltration as volume control. *Korean Circ J*. 2021;51(8):656–67.
- Ronco C, Ricci Z, Bellomo R, Bedogni F. Extracorporeal ultrafiltration for the treatment of overhydration and congestive heart failure. *Cardiology*. 2001;96(3–4):155–68.
- Costanzo MR. Ultrafiltration in Acute Heart failure. *Card Fail Rev*. 2019 Feb;5(1):9–18.
- Costanzo MR, Ronco C, Abraham WT, Agostoni P, Barasch J, Fonarow GC, et al. Extracorporeal Ultrafiltration for Fluid overload in Heart failure: current status and prospects for further research. *J Am Coll Cardiol*. 2017;69:2428–45.
- Lorenzin A, Neri M, Garzotto F, Ronco C. Solute and Water Kinetics in Continuous Therapies. *Critical Care Nephrology: Third Edition*. Elsevier 2019;1000–1005.e1.
- Neri M, Villa G, Garzotto F, Bagshaw S, Bellomo R, Cerda J, et al. Nomenclature for renal replacement therapy in acute kidney injury: basic principles. *Crit Care*. BioMed Central Ltd 2016.
- Claire-Del Granado R, Clark WR. Continuous renal replacement therapy principles. *Semin Dial John Wiley and Sons Inc*. 2021;34:398–405.
- Joannidis M, Oudemans-van Straaten HM. Clinical review: patency of the circuit in continuous renal replacement therapy. *Crit Care*. 2007.
- Murugan R, Hoste E, Mehta RL, Samoni S, Ding X, Rosner MH, et al. Precision Fluid Management in Continuous Renal Replacement Therapy. *Blood Purif*. S. Karger AG. 2016;42:266–78.
- Bouchard J, Mehta RL. Volume management in continuous renal replacement therapy. *Semin Dial*. 2009;22:146–50.
- Fiaccadori E, Parenti E, Regolisti G, Detrenis S. Ultrafiltrazione ed emofiltrazione nel paziente cardiologico. *G Ital Cardiol (Rome)*. 2010;11:104–20.
- Ronco C. Hemodiafiltration: Technical and Clinical Issues. *Blood Purif*. Karger S AG. 2015;2–11.
- Ejaz AA, Komorski RM, Ellis GH, Munjal S. Extracorporeal circuit pressure profiles during continuous venovenous haemofiltration. *Nurs Crit Care*. 2007;12:81–5.
- Michel T, Ksouri H, Schneider AG. Continuous renal replacement therapy. *Curr Opin Crit Care*. 2018;24:455–62.
- Yartsev Alex. Ultrafiltration as a mechanism of fluid removal. *Deranged Physiology, CICM Primary Exam - Required Reading, Renal system*. 2015. Available from: <https://derangedphysiology.com/main/cicm-primary-exam-required-reading/renal-system/dialysis-and-plasmapheresis/Chapter%20113/ultrafiltration-mechanism-fluid-removal>.
- Ficheux A, Ronco C, Brunet P, Argilés F. The ultrafiltration coefficient: this old “grand inconnu” in dialysis. In: *Nephrology Dialysis Transplantation*. Oxford University Press 2015. pp. 204–8.
- David S, David Nefrologia SU. Storia e principi biofisici, generali delle tecniche convettive. *G Ital Nefrol*. 2012;29(S55):3–11.
- CENELEC - European Committee for Electrotechnical Standardization. Medical electrical equipment Part 2: Particular requirements for basic safety and essential performance of haemodialysis, haemodiafiltration and haemofiltration equipment. 2018. Available online: https://webstore.iec.ch/preview/info_iec60601-2-16%7Bed5.0.RLV%7Den.pdf.
- Ali Ostadfar. Chapter 5 - Biofluid Flow in Artificial, Assistive and Implantable Devices. In: Ali Ostadfar, editor. *Biofluid Mechanics*. 2016.
- Alastair Campbell Ritchie. Chapter II.5.5 - Extracorporeal Artificial Organs. In: *Biomaterials Science (Third Edition)*. 2013. p. 827–41.

Publisher's Note Springer Nature remains neutral with regard to jurisdictional claims in published maps and institutional affiliations.